Some Interfacial Interactions between Isocyanates and Metals that Affect Release in Composite Wood-Panel Production*

Christopher Phanopoulos Servaas Holvoet Daniele Pratelli
Griet Pans Kyoko Shimizu Simon Ng
Jorge Bañuls-Ciscar Marie-Laure Abel John F. Watts

Abstract

Isocyanate- and polyurethane-based adhesives for composite wood-panel production are well known. They are useful for the manufacture of high-performance assemblies, particularly for moisture resistance, durability, and strength. However, isocyanate-based adhesives have several opportunities for improvements related to composite panel manufacture. Of particular note is the ability of isocyanates to bond, not only to wood, but to metal press platens used to produce the composite panels. Although several methodologies exist to overcome this, there is a lack of understanding of the nature of the interactions between isocyanates and metal. The purpose of the current study was to provide insights into these interactions and to help to develop strategies for releasable isocyanate-based resins.

Variable-thickness isocyanate–metal and metal–wood assemblies were prepared and the interface exposed by various methods, e.g., surface analysis combined with cluster beam etching and simple peel tests. The interfaces were then analyzed by X-ray photoelectron spectroscopy or time-of-flight–secondary ion mass spectrometry (or both). These surface analytical methods have revealed several chemical interactions between the isocyanates and the metal surfaces, including carbamate-type links and metal–nitrogen linkages. Further, the surface analysis has revealed the compositional character of the locus of failure in wood–metal joints. The locus of failure depends on the presence of wood extractives. With nonextracted wood, the locus of failure is within the wood, which is characterized by a certain concentration of the penetrated resin. With solvent-extracted wood, the locus of failure is within the glue line.

Isocyanate- and polyurethane-based adhesives and binders are extensively utilized for the preparation of composite wood assemblies in general and panels in particular. Isocyanate-based binders are efficient and are high-performance adhesives for wood. Even at very low loadings of 2 percent or less, high-strength, high-moisture-resistant composite panels are possible (Grunwald 2014). This high performance has resulted in a rapid growth of

The authors are, respectively, Senior Research Manager, Technical Manager Adhesives & Coatings, Application Specialist, and Senior Research Scientist, Huntsman Polyurethanes, Global Res., Everslaan, Everberg, Belgium (chris_phanopoulos@huntsman.com [corresponding author], servaas_holvoet@huntsman.com, daniele_pratelli@huntsman.com, griet_pans@huntsman.com); and PhD Student, PhD Student, PhD Student, Senior Research Fellow, and Professor of Materials Science, Surface Analysis Lab., Dept. of Mechanical Engineering Sci., Univ. of Surrey, Guildford, Surrey, UK (KShimizu@sacheminc.com, simon.onmun.ng@googlemail.com, j.banuls@surrey.ac.uk, m.abel@surrey.ac.uk, j.watts@surrey.ac.uk). Kyoko Shimizu is currently Senior Scientist, SACHEM Japan GK, Mizuhai, Higashi Osaka, Osaka, Japan. Simon Ng is currently Assistant to Chief Engineer (Corrosion and Assets), United Kingdom Atomic Energy Authority, Culham Centre for Fusion Energy, Abingdon, Oxon, UK. Jorge Bañuls-Ciscar is currently Project Officer, JRC European Commission. Marie-Laure Abel is currently Visiting Research Fellow, University of Surrey. This paper was received for publication in November 2017. Article no. 17-00078.

* This article is part of a series of eight selected articles addressing a theme of efficient use of wood resources in wood adhesive bonding research. The research reported in these articles was presented at the International Conference on Wood Adhesives, held on October 25–27, 2017, in Atlanta, Georgia. All eight articles are published in this issue of the *Forest Products Journal* (Vol. 68, No. 4).

Forest Prod. J. 68(4):390–397.
doi:10.13073/FPJ-D-17-00078

isocyanates and polyurethanes in this application area, particularly in oriented strand board (OSB) and medium-density fiberboard. In addition to the excellent performance of isocyanate-bonded wood, there are several production-related benefits, e.g., the requirement for low levels of resin stock, the stability of the resin during storage, the wide species and waste wood furnish tolerance, and the high moisture content tolerance of the to-be-bonded wood. The latter means lower energy consumption for drying, less thermal wood damage, reduced potential for fires, better control of the ex-press moisture content, and consequently a lower reject rate.

However, there is one aspect of isocyanate-bonded wood manufacture that still could be improved. Isocyanates and polyurethanes not only bond well to wood, but also to metals. This can lead to press platen or press belt fouling and consequently production downtime for cleaning. Further, the adhesion strength between the isocyanate and the metal can sometimes be greater than the cohesive strength of the wood and consequently the panels that are in preparation can be torn apart. Preventing the adhesion to the press is therefore vital for the manufacturing process. Fortunately there are several methods that can be used to overcome this issue. Examples of such methods include the following.

1. Use of multilayer panels in which the outer faces of the panel are bonded to a sacrificial layer, such as unbonded wood or urea-formaldehyde–bonded wood. This layer can be readily removed by sanding.
2. Use of external release agents. Release agents (usually waxes or soaps) are sprayed onto the belts (continuous presses) or on the bottom plate and the top of the prepressed panel (multiday light presses), providing a barrier layer, preventing adhesion to the press. This method is successfully used in several manufacturing facilities. However, spraying such release agents can have hygiene issues, can be costly, can be ineffective when strand flipping occurs, can compromise the subsequent physicomechanical performance of the panel, and can affect postmanufacturing processes.
3. Use of internal release agents. There are several versions of internal release agents commercially available; again these may affect the physicomechanical performance and can be costly.

Therefore there remains an opportunity to improve the manufacturing process of isocyanate-bonded composite wood panels. It is the purpose of the current research to try to elucidate the nature of the metal–isocyanate interface so as to help develop novel strategies to prevent, with cost-effective and efficient means, the adhesion to the press during the manufacture of composite wood panels.

Others have also studied metal isocyanate interactions. Dillingham and Moriarty (2003) studied the interfacial interaction between isocyanate-based polymers and steel using Fourier transform infrared reflective spectroscopy. They found evidence for a reaction between the NCO group and hydrated oxide layers, leading to metal-carbamate–type reaction products. Chehimi and Watts 1992 studied the interfacial reactions of aromatic moisture-cured urethanes and steel using X-ray photoelectron spectroscopy (XPS). They determined that there is a change in the oxide state of iron when moisture-cured urethanes are deposited on the metal; this change was consistent with the formation of a reaction of the surface hydroxyl groups with the isocyanate. Kim et al. (2005) studied the variation of the electrochemical potential between a urethane reacting system and aluminum and proposed the formation of a stable carbamate link between the isocyanate and aluminum. Still later Shimizu et al. (2012, 2013), using XPS and secondary ion mass spectrometry (STATIC-SIMS), investigated the interactions of isocyanates with various metals, including iron, aluminum, chromium, copper, and steel. Shimizu (2011) found that moisture on the surface of metals reacts to generate urea groups. She also found the presence of a covalent link with aluminum, namely $ALCHNO_3^-$, indicating a carbamate-type link. Finally Shimizu et al. (2013) postulated acid–base interactions between iron surfaces and isocyanates. Nies et al. (2012) and Fug et al. (2014) also demonstrated, by a series of washing steps, that isocyanates on metals form stable chemical bonds, whereas the ureas that are formed, because of the reaction of isocyanates with surface moisture, gave rise to physically adsorbed species.

These types of interactions need to be studied in more detail and in the presence of wood to understand the nature of the interactions in full. This article reviews some of the work that has been done by the authors over the last few years as well as introducing some of the most recent work.

Experimental

Sample preparation of variable-thickness coated metals was done in the following way. Iron or aluminum (Rocholl, 99.5% pure) strips were washed in an ultrasonic bath in acetone (Aldrich). Variable concentrations (0.05% to 5%, wt/wt) of SUPRASEC 5025 isocyanate from Huntsman in acetone (Aldrich) were then spin cast on the plates. The coated metals were then allowed to cure at 200°C for several minutes in the case of the iron samples or at ambient temperature in the case of the aluminum substrates, after which the quality of the surface and interface was investigated by time-of-flight (ToF)–SIMS.

Alternatively, for the depth-profiling experiments, silicon wafer squares of 10 by 10 mm^2 were cut using a diamond scribe and subsequently cleaned with acetone using an ultrasonic bath to remove any surface contamination. Immediately after, samples were transferred to a sputter coater where thick metal coatings were applied using an iron–chromium target. The nominal composition of the coating (determined by energy-dispersive X-ray spectroscopy) was $Fe_{0.8}Cr_{0.2}$. SUPRASEC 5025 polymeric methylene diphenyl diisocyanate (pMDI) solutions of 0.05 and 1 percent (by weight) in acetone were prepared to produce pMDI coatings with different thicknesses. Coatings were sprayed on the metal substrates and immediately transferred to an oven set at 200°C to be cured.

Pinus sylvestris strands, provided by an Eastern European OSB producer, were either used as received or after a series of solvent extractions (dichloromethane, toluene-ethanol, ethanol, acetone; all supplied by Aldrich) using a Soxhlet apparatus. In both cases the wood was stored for at least 1 week in a Weiss cabinet at 22°C and 55 percent relative humidity before use. Steel foil strips (Berndorf band steel, NICRO 52.6 to 50 μm thick and 20 mm wide) were acetone washed before use. Single drops of known mass (0.005, 0.015, or 0.030 g) of SUPRASEC 5025 pMDI were applied

at discrete points along the wood strands and the metal strips were then placed over the resin droplets and the assembly was pressed and cured in a Servitec Polystat 200T laboratory press at 200°C for 2 minutes. The joints were then tested to failure in peel mode using an Instron 5566 universal testing instrument. The cross-head speed was 50 mm/min, the peel angle was 180°, and the curve of the peel was controlled by placing a rod 1.3 cm in diameter at the point of failure. The variable-thickness pMDI-coated metals and the failed joint surfaces were then analyzed by XPS or ToF-SIMS (or both).

ToF-SIMS analyses were performed using a TOF.SIMS 5 (ION-TOF GmbH, Munster, Germany) equipped with C_{60}^+ sputter source. Both positive and negative ions were collected using 25 keV Bi_3^+ as primary ion beam. Spectra were acquired under static conditions, the primary ion beam rastered in random mode over an area of 100 by 100 μm^2. Depth profiles were performed by raster scanning an area of 200 by 200 μm^2 at the center of the crater sized 600 by 600 μm^2 formed by the C_{60}^+ sputter beam.

ToF-SIMS depth profile data sets were processed using the SurfaceLab software (ION-TOF GmbH). Spectra were calibrated using a unique mass calibration list, and the peak list with areas of the approximately 700 most intense peaks was obtained using the peak search tool. Subsequently, secondary ion images were reconstructed for all previously selected peaks at each depth profile level. The data were then exported as binary BIF6 files.

The software used to perform nonnegative matrix factorization (NMF) was the simsMVA app (Trindade 2017) developed at the University of Surrey. BIF6 files were loaded into the three-dimensional (3D) mode of simsMVA to carry out NMF as described by Trindade et al. (2017), using the algorithm of Lee and Seung (2001). Data were normalized by total ion intensity, Poisson scaled, and three components were chosen to perform NMF. NMF analysis provided a characteristic spectrum of each component and a 3D visualization of the data set, showing the spatial distribution of the intensities of the three NMF components.

XPS analyses were carried out in a Thermo Scientific K-Alpha$^+$ spectrometer using an Al K_α monochromatic X-ray source and an argon cluster (MAGCIS) sputter source. An electron flood gun was used to compensate for the electron deficiency in the analyzed area. The spot size used for analysis was 400 μm in radius. The pass energy and step size for high-resolution spectra acquisition was 50 and 0.2 eV, respectively (Bañuls-Ciscar et al. 2016).

Results and Discussion

Figure 1 shows schematically the nature of the variable coating thicknesses of isocyanate on metal surfaces (Shimizu 2011). Surface analysis of the thicker layers (Fig. 1b) gives information about the upper surface of the cured isocyanate and some limited information about the bulk layer of the isocyanate (the quality and quantity of information from the bulk depend on the setup of the ToF-SIMS instrument). For the thickest layers of isocyanate on metal, the detected mass fragments are effectively the same as for a detached film of isocyanate (Fig. 1a). However, when the film becomes thin enough, the depth of analysis is sufficient to start observing fragments from the interface of the isocyanate on the metal (Fig. 1c). When the isocyanate layer is still thinner (Fig. 1d), surface and interface can be analyzed easily and there is little, if any, ''interference'' of bulklike material.

The surface of the detached film or coated layers of isocyanate on metals reveals several mass fragments characteristic of moisture-cured isocyanates (Shimizu 2011). These include mass/charge = 106, which is assigned to

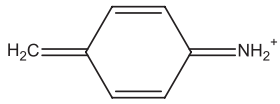

and from the subsurface fragments such as:

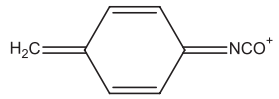

at a mass/charge = 132 u.

The spectra showing these fragments can readily be seen in Figure 2 (Shimizu 2011).

Fragments generated from the interface were found to be similar to those on the surface of the isocyanate layer, i.e., typical of moisture cure, even when the bulk material was showing uncured material. This suggests that the interfacial isocyanate was reacting with metal surface moisture to form urea-type moieties.

Magnifying and analyzing the high-mass resolution spectra reveal more information about the interfacial region. As an example, upon observation of the isocyanate–aluminum interface, a series of mass/charge fragments in the negative ion spectrum are seen at around 102 u (see Fig. 3).

As can be seen, in this series of spectra, as the isocyanate layer becomes thinner, an interfacial fragment is revealed that is different from either an isocyanate fragment or a metal fragment all at around the same mass. Hence, on the thick isocyanate layer, an isocyanate-origin fragment assigned to $C_7H_4N^-$ (mass = 102.1134 u) is observed. On the bare aluminum surface a mass fragment assigned to $Al_2O_3^-$ (mass = 101.9613 u) is observed (as well as a second fragment assigned to $C_2O_2Na_2^-$ [mass = 101.9997 u]). As the isocyanate layer becomes increasingly thinner, a new fragment is seen between the isocyanate-origin and aluminum-origin fragments. This new fragment has been assigned to $AlCHNO_3^-$ (mass = 102.0051 u). This new fragment is clearly a mixed organic-metal fragment, indicative of strong bonding between the isocyanate and the metal. It is unclear if this is an ionic or covalent link, and no literature was found to indicate preferences for either.

The accuracy of the assignment can be seen from the difference in the theoretical mass of the proposed fragment and that of the experimental measurement. High confidence is achieved when the mass difference (identified as the Δ parameter) is less than 100 ppm. The differences in the assignments are shown in Table 1 below.

The Δ parameter, the difference in mass (relative to the theoretical), is very low and therefore the confidence in the assignment is high. The schematic below shows where the interfacial fragment could originate from:

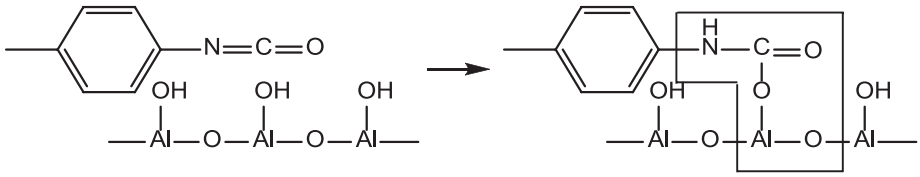

Similar fragments, albeit at other masses, were seen for Fe–isocyanate interfaces and Cr–isocyanate interfaces (Shimizu 2011). Such fragments are in agreement with Dillingham and Moriarty (2003) in that interactions with surface hydroxyl groups to form urethane or carbamate-type links are observed.

When the interface is further studied (Bañuls-Ciscar et al., submitted for publication) by depth profiling and the spectra data investigated using NMF, different types of interactions that are less expected are observed. It was possible to separate the depth profile data sets into spectra typical of the outer surface, the interface, and the metal substrate. The spectrum of the outer surface corresponds to that of characteristic fragments of pMDI (Shimizu et al. 2010). The spectrum of the pMDI–Fe interface was further investigated to obtain more information of the interfacial chemistry.

A series of significant fragments of masses 130.934, 158.978, 159.974, and 319.985 u were found and assigned to $CHNO_3Fe^-$, $C_7H_5NFe^+$, $C_7H_6NFe^+$, and $C_{15}H_8N_2O_3Fe^+$. Assignments with their deviation and proposed structure are shown in Table 2. Again, the deviation of the theoretical to measured masses was very low, confirming the fidelity of the assignments.

Table 1.—Difference in mass of the assigned fragments seen in Figure 3 compared with the theoretical mass of those fragments.

Assigned fragment	Experimental mass (u)	Exact mass (u)	|Δ| (ppm)
$Al_2O_3^-$	101.9434–101.9506	101.9478	6.9–43.2
$AlCHNO_3^-$	101.9758–101.9793	101.9772	3.9–20.6
$C_2O_2Na_2^-$	101.9683	101.9694	10.8
$C_7H_4N^-$	102.0289–102.0364	102.0344	2.9–53.9

The assignments suggest that pMDI is reacting with iron through two reaction mechanisms. The first is similar to that proposed above (Dillingham and Moriarty 2003), where the NCO group reacts with surface hydroxyls to form carbamate-type links. Second, after reaction of the NCO group with water on the surface of the metal, generating the aromatic amine, this then reacts with an iron atom by donating a pair of electrons and creating a metal–N bond. XPS would expect to show an N–metal-type link in the N1s high-resolution spectrum and indeed it does, as reported by Bañuls Ciscar et al. (submitted for publication). XPS and SIMS do not provide information about the nature of the metal–N bond, e.g., whether they are more ionic or covalent in nature. This may be the focus of future studies.

The above studies have revealed the potential strong and stable bonds responsible for the adhesion process between isocyanates and metals (in this case an iron–chromium alloy). During composite wood manufacture, there are several further complicating components to consider. The press is usually much hotter than the temperatures at which the above studies were conducted. Further, wood and wood extractives and moisture are present, all of which are potentially very reactive toward the isocyanates. The quality of the press platen surfaces could be considerably different because of oxidative and erosion processes. It is important therefore to mimic the real situation more closely so as to increase confidence that the above reactions are happening during the real production process.

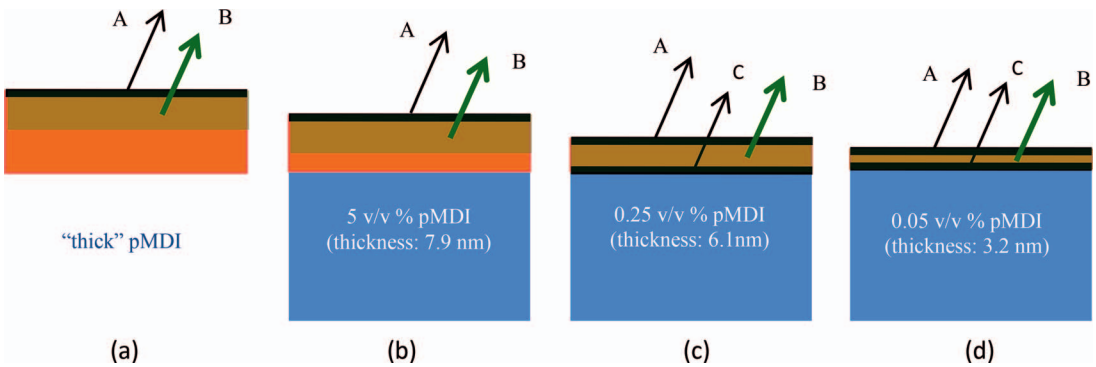

Figure 1.—Schematic of variable-thickness layers of isocyanate on a metal substrate. Time-of-flight–secondary ion mass spectrometry analysis of the detached adhesive–isocyanate film (a) reveals fragments from the surface (A) of the cured isocyanate and some information from the subsurface (B). The same mass spectrum (A and B) is seen for thick layers of isocyanate on metals (b). However, as the film thickness is diminished (c), mass fragments from the interface (C) start to be seen in addition to the fragments from the isocyanate surface (A) and subsurface (B). Still thinner isocyanate layered samples (d) reveal clearer surface (A) and interface (C) fragments. pMDI = polymeric methylene diphenyl diisocyanate. (Color version is available online.)

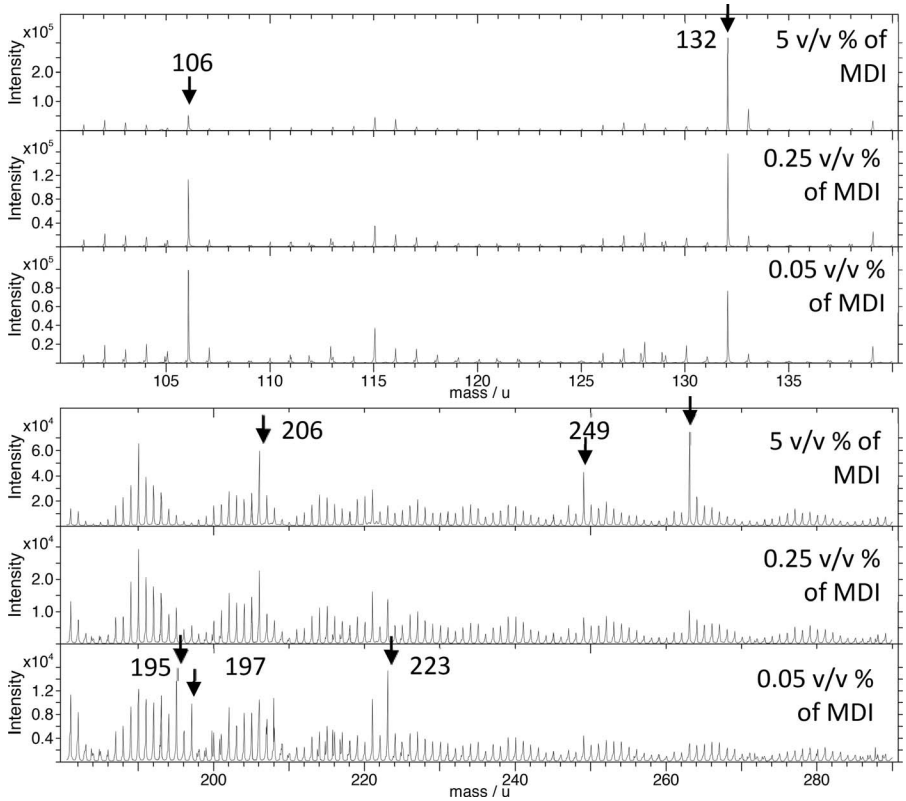

Figure 2.—Positive time-of-flight–secondary ion mass spectrometry spectra of methylene diphenyl diisocyanate (MDI) solution in the range of 5 to 0.05 percent (vol/vol) coated on degreased iron.

Table 2.—Proposed structures of the fragments from the interface between polymeric methylene diphenyl diisocyanate and the metal substrate.

Mass (u)	Assigned formula	Mass deviation (ppm)	Proposed structure
130.932	$CHNO_3Fe^-$	21.4	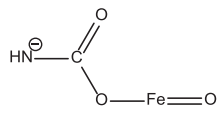
158.978	$C_7H_5NFe^+$	33.8	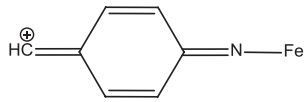
159.974	$C_7H_6NFe^+$	35.5	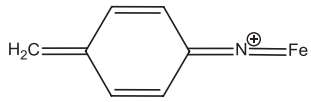
319.985	$C_{15}H_8N_2O_3Fe^+$	41.0	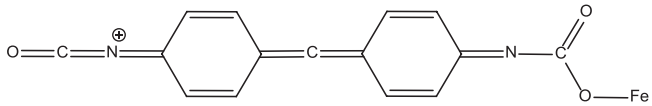

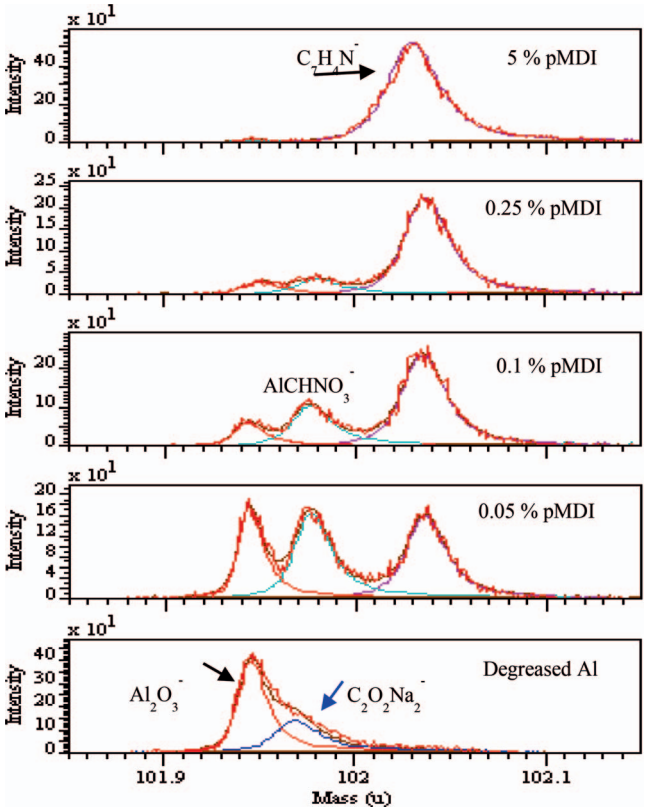

Figure 3.—Magnified negative-ion high-resolution mass spectra of isocyanate, aluminum, and isocyanate-coated aluminum (various thicknesses) centered around a mass of 102 u. pMDI = polymeric methylene diphenyl diisocyanate.

During pressing, should there be any lack of release (which of course happens when no release agent is used), the above proposed mechanisms of adhesion would be strong enough to cause failure within the composite wood panel and hence the creation of bound debris on the press platens. It is important to understand the nature of this failure. To this end, surface analytical studies have been undertaken to understand the locus of failure during the pressing of isocyanate–wood composites.

As described above, a series of wood–metal foil samples was prepared by gluing the two substrates (metal and wood, extracted or nonextracted) with isocyanate resins. The assemblies were then failed by application of a 180° peeling force. The failure load was noted and the exposed surfaces were analyzed by XPS.

Figure 4 shows the load required to cause failure for extracted and nonextracted wood–metal joints. As can be seen, the failure loads for the nonextracted wood is of the order of 1.4 to 1.8 N, irrespective of the volume of resin droplet used to effect adhesion. For extracted wood, again, the droplet size does not have an impact, but the failure load is reduced to 0.8 to 1.1 N. Further, in the case of the nonextracted wood, there is a large amount of residual wood debris remaining of the metal foil, whereas in the case of extracted wood, there is far less debris.

The XPS analyses of the failed assemblies focused on the nitrogen content of the exposed surfaces. The results of this are shown in Figure 5. As can be seen, for the nonextracted wood systems, the amount of nitrogen on the failed surfaces is constant at around 4 percent. The results for the intermediate isocyanate droplets are not shown, but were found to be the same. For the extracted wood, however, the small droplet system (and the mid-size droplet system, not shown) revealed a much higher nitrogen content, at around 10 percent. The larger droplet system, with extracted wood, showed a locus of failure with a similar nitrogen content to that of the nonextracted wood, i.e., at a nitrogen content of around 4 percent.

That this is a true locus of failure was checked by conducting analysis across the metal–wood interface to see if there was a concentration gradient. Such a gradient was indeed determined, as shown in Figure 6.

Thus it can be seen that steel–wood bonds do indeed fail at a point where there is a certain concentration of nitrogen (when the nitrogen is provided by isocyanate resins); thus the true locus of failure has been determined. This locus of failure is at the point where there is 4 percent nitrogen for nonextracted wood and 10 percent nitrogen for extracted wood (and again 4 percent nitrogen for extracted wood when there is an abundance of isocyanate).

Four percent nitrogen relates to an isocyanate loading of ca. 30 percent, and 10 percent nitrogen relates to an isocyanate loading of ca. 100 percent. Thus, in the case of the nonextracted wood, the failure is happening at a point in the wood where the isocyanate has penetrated and where the dilution of the isocyanate has reached 30 percent. This sounds like a high isocyanate loading. Those familiar with the use of isocyanates in composite wood will know that resin loadings of 2 to 4 percent are very commonly used. However, the cited 30 percent isocyanate at the point of failure is not a contradiction. In gluing wood composites with isocyanates, discrete droplets of the resin are distributed over the surface of the wood. At the points where the droplets touch the wood, the resin loading is very high. However, there is a large amount of wood that does not see any isocyanate; thus, there is a low overall loading of resin, but at the points where resin droplets are found, the resin concentration is high.

For the extracted wood, the 10 percent nitrogen equates to 100 percent isocyanate. Hence, with extracted wood, the assembly is showing cohesive failure in the glue line. This is not unexpected since it is known (Phanopoulos 2010) that extractives can leach out of wood into the isocyanate where they react, forming a range of products, including urethane-linked products. These urethanes toughen the otherwise strong but brittle polyurea, which is formed during the curing of isocyanates with moisture (Bao et al. 1999). In the absence of the extractives, such bonds do not form and the brittle behavior of the polyurea dominates. Hence the difference in locus of failure of the extracted and nonextracted wood assemblies. But why does the high resin droplet extracted system show a 4 percent nitrogen locus of failure? It is speculated that the larger droplet size of the resin allows for deeper penetration of the resin into the wood, which potentially accesses extractives that have failed to be removed and therefore, the toughened glue line is again possible.

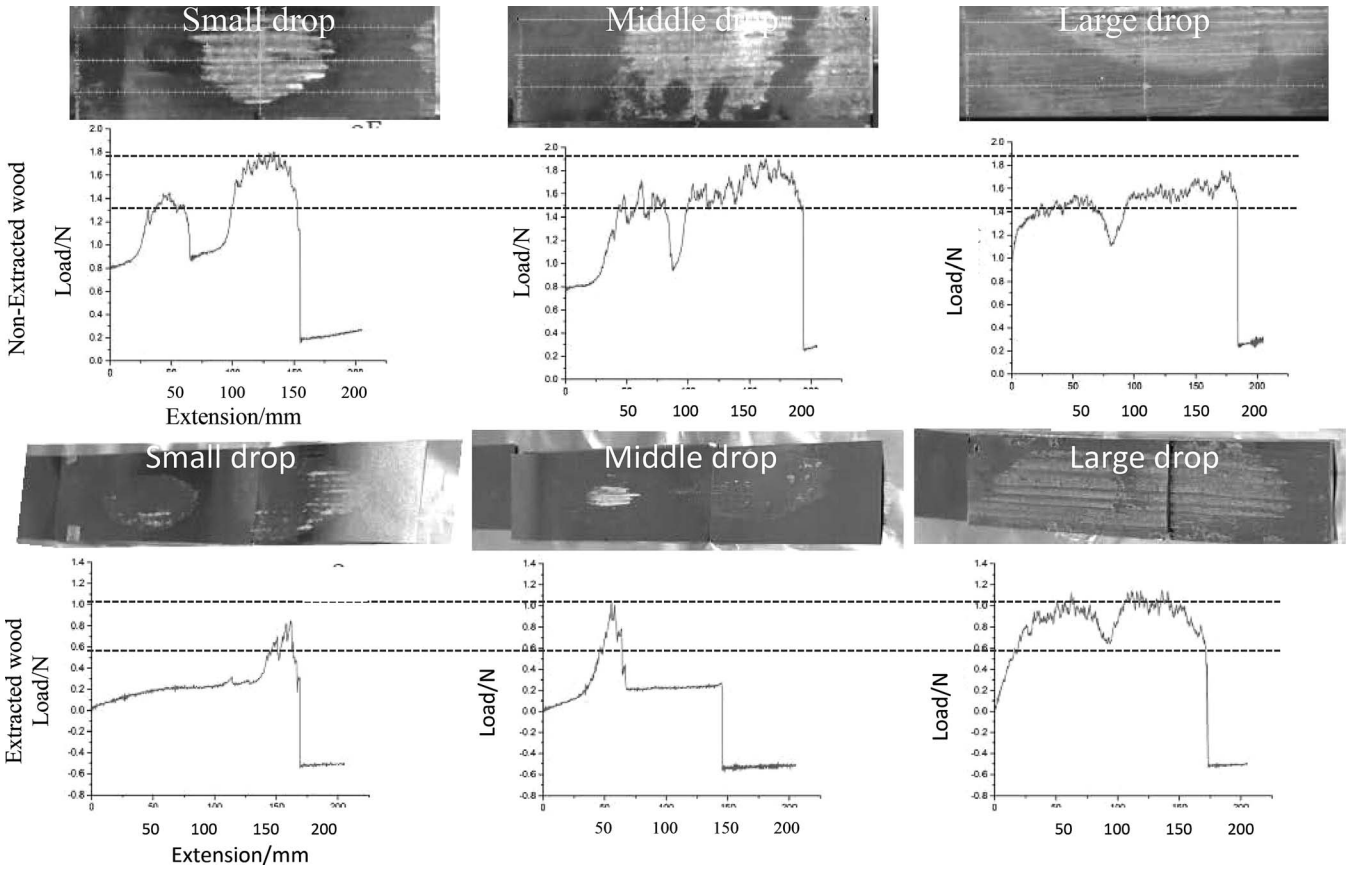

Figure 4.—Failure loads of 180° peel tests of steel foil–extracted and nonextracted wood assemblies using a range of isocyanate loadings, together with photographs of the steel failure surfaces. The vertical field of view is approximately 20 mm (the width of the foils). Small, middle, and large drops refer to drops of 0.005, 0.015, and 0.03 g, respectively. In each case, pairs of equal-weight drops were placed along the piece of wood to achieve pairs of discrete bonding areas in the assembly.

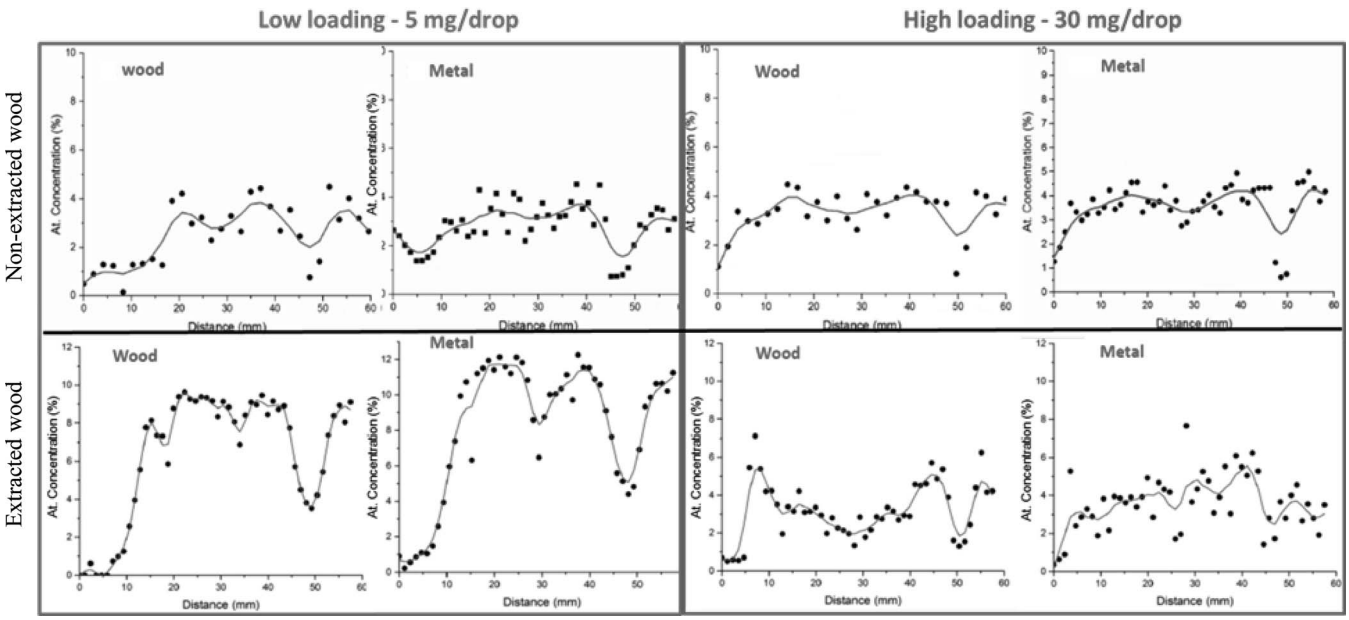

Figure 5.—Nitrogen content measured by X-ray photoelectron spectroscopy on failed surfaces of steel foil–extracted and nonextracted wood assemblies (various isocyanate loadings) failed under 180° peel tests.

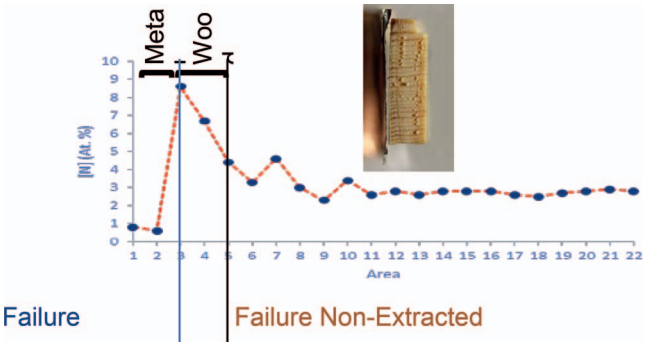

Figure 6.—Composite diagram indicating the nitrogen concentration (measured by energy-dispersive X-ray spectroscopy) across the steel foil–wood interface of several peel test assemblies (a photograph of the prefailed sample is shown in the insert to illustrate the analyzed interface). The abscissa can be considered as depth, progressing from the outer regions of the metal substrate (Points 1 and 2) moving into the bulk of the wood. The lines indicate the loci of failure of nonextracted wood systems (black) and low isocyanate-bonded extracted wood systems (blue).

Conclusions

XPS and ToF-SIMS have revealed that carbamate-type links between isocyanates and metal surfaces (via the metal hydroxide groups) are formed. Depth profiling using ToF-SIMS in conjunction with multivariate analysis has revealed that metal–N bonds are also formed at the isocyanate–metal interface. It is speculated that hydrolysis of the NCO group with moisture that is bound to the metal surface to generate the corresponding amine is the first step in the adhesive bond formation, followed by the nitrogen of the amine bonding directly to the metal via lone-pair donations. Both the carbamate and metal–N links are strong, and are at least partially responsible for the strong adhesion and potential fouling of the metal plates in the press during composite wood manufacture.

Because the interfacial bonds are strong, they would induce failure elsewhere in the metal–wood assembly when the system is strained. The failure seems to be inside the wood where the nitrogen content is at the 4 percent level. This seems an important aspect worthy of further investigation so as to determine the nature of the isocyanate–wood morphology at this particular composition. The wood extractives do seem to play an important role in inducing the failure at the 4 percent nitrogen level. In the absence of the wood extractives, the assemblies seem to fail cohesively in the brittle, moisture-cured polyurea glue line.

Acknowledgment

The authors thank Gustavo Ferraz Trindade (originator of the simsMVA app) for advice and support in the use of the NMF software.

Literature Cited

Bañuls-Ciscar, J., D. Pratelli, M.-L. Abel, and J. F. Watts. 2016. Surface characterization of pine wood by XPS. *Surf. Interface Anal*. 48:589–592.

Bañuls-Ciscar, J., G. F. Trindade, M.-L Abel, D. A. Jesson, C. Phanopoulos, G. Pans, D. Pratelli, K. Marcoen, T. Conard, and J. F. Watts. A study of the interfacial chemistry between polymeric MDI and Fe/Cr alloy. (Submitted for publication.)

Bao, S.; W. A. Daunch, Y. Sun, P. L. Rinaldi, J. J. Marcinko, and C. Phanopoulos. 1999. Solid state NMR studies of pMDI derived species in wood. *J. Adhes*. 71(4):377.

Chehimi, M. M. and J. F. Watts. 1992. An XPS study steel–aromatic moisture-cured urethane interface. *J. Adhes. Sci. Technol*. 6:377–393.

Dillingham, R. G. and C. Moriarty. 2003. The adhesion of isocyanate-based polymers to steel. *J. Adhes*. 79:269–285.

Fug, F., C. Nies, and W. Possart. 2014. In situ FTIR study of adhesive interactions of 4,4′methylene diphenyl diisocyanate and native metals. *Int. J. Adhes. Adhes*. 52: 66–76.

Grunwald, D. 2014. Wood based panels with enhanced properties: What is possible with MDI today? 9th European Wood Based Panels Symposium, October 10, 2014, Hanover.

Kim, J., J. Cho, and Y. S. Lim. 2005. Bonding of urethane reactants to aluminium surface. *J. Mater. Sci*. 40(11):2789–2794.

Lee, D. and H. Seung. 2001. Algorithms for nonnegative matrix factorization. *Adv. Neural Inf. Process. Syst*. 1:556–562.

Nies, C., C. Wehlack, H. Ehbing, D. J. Dijkstra, and W. Possart. 2012. Adhesive interactions of polyurethane monomers with native metal surfaces. *J. Adhes*. 88(8):665–683.

Phanopoulos, C. 2010. Polyurethanes and Isocyanates Used as Adhesives in Composite Wood Products: A Monograph. 2nded.Huntsman Corporation, The Woodlands, Texas.

Shimizu, K. 2011. The characterization of interfacial interactions between MDI and metal substrates. PhD thesis. University of Surrey, UK.

Shimizu, K., M. L. Abel, C. Phanopoulos, S. Holvoet, and J. F. Watts. 2012.The characterization of the interfacial chemistry of adhesion of rigid polyurethane foam to aluminium. *J. Mater. Sci*. 47:902–918.

Shimizu, K., M. L. Abel, C. Phanopoulos, S. Holvoet, and J. F. Watts. 2013. A TOF-SIMS investigation of the thermodynamics and bonding of polymeric methylene diphenyl diisocyanate on oxidized aluminium and iron surfaces. *RSC Adv*. 3(27):10754–10763.

Shimizu, K., C. Phanopoulos, R. Loenders, M.-L. Abel, and J. F. Watts. 2010. The characterization of the interfacial interaction between polymeric methylene diphenyl diisocyanate and aluminum: a ToF-SIMS and XPS study. *Surf. Interface Anal*. 42:1432–1444.

Trindade, G. F. 2017. simsMVA.pdf [online]. https://mvatools.com/. Accessed October 2016.

Trindade, G. F., M.-L. Abel, and J. F. Watts. 2017. Non-negative matrix factorisation of large mass spectrometry datasets. *Chemom. Intell. Lab. Syst*. 163:76–85.